eprints@whiterose.ac.uk
https://eprints.whiterose.ac.uk/

Can planet–planet binaries survive in star-forming regions?

Richard J. Parker[*][†], Simon P. Goodwin and Jessica L. Diamond
Astrophysics Research Cluster, School of Mathematical and Physical Sciences, The University of Sheffield, Hounsfield Road, Sheffield, S3 7RH

ABSTRACT

Significant numbers of free-floating planetary-mass objects have been discovered in nearby star-forming regions by the James Webb Space Telescope, including a substantial number (42) of Jupiter Mass Binary Objects ('JuMBOs') in the Orion Nebula Cluster. The JuMBOs have much wider separations than other populations of substellar binaries, and their existence challenges conventional theories of substellar and planetary-mass object formation. Whilst several theories have been proposed to explain their formation, there has yet to be a study that determines whether they could survive the dynamical encounters prevalent within a dense star-forming region. We place a population of planet–planet binaries in *N*-body simulations of dense star-forming regions and calculate their binary fraction over time. We find that between 50 – 90 per cent of planet–planet binaries are destroyed on timescales of a few Myr, which implies that many more must form if we are to observe them in their current numbers. Furthermore, if the ONC was much more dense at formation, the initial separation distribution of the JuMBOs must have been even wider (and less similar to other substellar binaries) than the observed distribution.

Key words: stars: formation – kinematics and dynamics – open clusters and associations: general – methods: numerical

1 INTRODUCTION

Understanding the boundary between stars and planets (or whether a boundary exists) is one of the most important topics in modern astrophysics, and is being revolutionised by the first data from the James Webb Space Telescope (JWST). In particular, JWST has discovered significant numbers of free-floating planetary-mass objects (McCaughrean & Pearson 2023; Langeveld et al. 2024; Luhman 2024; Luhman et al. 2024b,a).

Some of these substellar objects appear to be in binaries (Jupiter-Mass Binary Objects, or 'JuMBOs' for short, Pearson & McCaughrean 2023) with projected separations 28 – 384 au. These systems are unusually wide for substellar binaries (which typically have separations below 10 au, Burgasser et al. 2007; Thies & Kroupa 2007; Factor & Kraus 2023), and pose a challenge for formation theories.

The fidelity of the JuMBOs has been questioned by Luhman (2024) who finds that their colours are more consistent with reddened background sources, rather than young substellar objects in a star-forming region. In spite of this uncertainty, several theories have been proposed to explain them (Lazzoni et al. 2024; Portegies Zwart & Hochart 2024), ranging from liberation of pairs of planets from their parent stars (Wang et al. 2024) to photoerosion of the cores of systems that would otherwise go on to form much wider stellar-mass binaries (Whitworth & Zinnecker 2004; Diamond & Parker 2024).

The candidate JuMBOs were discovered in the Orion Nebula Cluster (ONC), the most dense star-forming region within 500 pc of the Sun (King et al. 2012), and many studies have demonstrated that stellar and substellar binaries are disrupted in star-forming regions with densities $\geq 100 \, M_\odot \, pc^{-3}$ (Kroupa et al. 1999; Parker & Goodwin 2011; Parker et al. 2011; Marks & Kroupa 2012; Parker 2023).

In this Letter, we investigate whether planet–planet binary systems can survive in dense star-forming regions, and what the implications of this are for the JuMBOs observed with JWST. We present our methods in Section 2, we present our results in Section 3 and we conclude in Section 4.

2 METHODS

We run *N*-body simulations of the dynamical evolution of star-forming regions in which we place a population of planet–planet binaries. The regions contain N_{sys} = 1500 systems – either a single star or a planet-planet binary system. For simplicity, the stellar systems are all single stars[1], with masses drawn from a Maschberger (2013) Initial Mass Function, which has a probability distribution for selecting a mass *m*

---

[*] E-mail: r.parker@sheffield.ac.uk
[†] Royal Society Dorothy Hodgkin fellow

---

[1] In the ONC the stellar binary fraction is similar to that in the Galactic field, ~50 per cent (King et al. 2012). If we were to include stellar binaries, the number of destructive encounters would likely be higher, due to the higher collisional cross section of the binaries compared to single stars (Li & Adams 2015; Li et al. 2020).

Table 1. Summary of simulation set-ups. The columns show the simulation label, the lower limit to the initial mass function for the single systems, m_{low}, the separation distribution for the planet–planet binaries, and the initial median local stellar density $\tilde{\rho}$ in the star-forming region.

Sim.	m_{low}	planet–planet separations	$\tilde{\rho}$
A	$0.08\,M_\odot$	JuMBOs $(28 - 384\,au)$	$10\,000\,M_\odot\,pc^{-3}$
B	$0.08\,M_\odot$	JuMBOs $(28 - 384\,au)$	$100\,M_\odot\,pc^{-3}$
C	$0.01\,M_\odot$	JuMBOs $(28 - 384\,au)$	$10\,000\,M_\odot\,pc^{-3}$
D	$0.08\,M_\odot$	$50 - 500\,au$	$10\,000\,M_\odot\,pc^{-3}$
E	$0.08\,M_\odot$	$50 - 500\,au$	$100\,M_\odot\,pc^{-3}$

of the form

$$p(m) \propto \left(\frac{m}{\mu}\right)^{-\alpha} \left(1 + \left(\frac{m}{\mu}\right)^{1-\alpha}\right)^{-\beta}. \tag{1}$$

In this equation, $\alpha = 2.3$ is the Salpeter (1955) slope describing the high-mass end of the IMF, and $\beta = 1.4$. $\mu = 0.2\,M_\odot$, and we adopt an upper limit to the IMF of $m_{up} = 50\,M_\odot$. In most of our simulations (A, B, D, E) we adopt a lower mass limit of $m_{low} = 0.08\,M_\odot$, i.e. we do not create a population of brown dwarfs that overlap in mass with the the JuMBOs. However, in one set (C) we adopt $m_{low} = 0.01\,M_\odot$ to create a population of single brown dwarfs.

We randomly select 10 per cent of the systems to be planet–planet binaries, and randomly draw their component masses from the JuMBO masses provided in Pearson & McCaughrean (2023). In three sets of simulations (A, B, C), we draw the separations of these binaries randomly from the JuMBO catalogue (we take the separation from the same system from which we draw the component masses), but in two sets (D and E) we draw them from a flat distribution between 50 - 500 au.

We do not have any information on the eccentricity of the observed JuMBO systems, and we therefore set all eccentricities to zero.

Observations (e.g. Gomez et al. 1993; Cartwright & Whitworth 2004; Sánchez & Alfaro 2009; Hacar et al. 2013; André et al. 2014) and simulations (e.g. Schmeja & Klessen 2006; Bate 2009; Girichidis et al. 2011; Dale et al. 2012) suggest that stars form in filamentary structures, which then converge to form hubs of star formation (Myers 2011), resulting in a spatially substructured distribution for the stars.

A convenient way of setting up N-body simulations with substructure is to use the box fractal method (Goodwin & Whitworth 2004), which has the advantage that the degree of spatial and kinematic substructure is described by just one number, the fractal dimension D. For a detailed description of the fractal set-up, we refer the interested reader to Goodwin & Whitworth (2004) and Daffern-Powell & Parker (2020). In three dimensions, a fractal with a high degree of substructure is created with $D = 1.6$, whereas a uniform sphere is produced when $D = 3.0$. Observed star-forming regions are all consistent with having evolved from much more substructured distributions (Daffern-Powell & Parker 2020) and we therefore adopt $D = 1.6$ in all of our simulations.

The velocities of the objects in the fractal distribution are set so that the velocity dispersion is small on local scales, but can be quite different on larger scales, similar to observations (Larson 1981; Hacar et al. 2013; Henshaw et al. 2016).

Observations and simulations also suggest that young stars are likely to have a low velocity dispersion with respect to the gravitational potential, i.e. be subvirial (Foster et al. 2015; Kuznetsova et al. 2015; Vázquez-Semadeni et al. 2019), and we scale the velocities to be subvirial ($\alpha_{vir} = 0.3$, where the virial ratio $\alpha_{vir} = T/|\Omega|$, and T and Ω are the total kinetic and potential energies of the objects, respectively).

We select two radii, r_F for the star-forming regions, such that our simulations encompass the full range of possible initial densities for the ONC. The present-day stellar density in the central regions of the ONC is several hundred $M_\odot\,pc^{-3}$ (King et al. 2012), and it is possible that the initial density was similar. However, 'reverse engineering' – the process of comparing properties of N-body simulations (such as the amount of spatial substructure, number of runaway and walkaway stars, degree of mass segregation, binary star orbital distributions) – suggests a much higher initial density, perhaps up to $10^4\,M_\odot\,pc^{-3}$ (Allison et al. 2010; King et al. 2012; Marks & Kroupa 2012; Parker et al. 2014; Parker 2014; Schoettler et al. 2020). To account for these two extremes, we adopt $r_F = 1\,pc$, and $r_F = 5\,pc$, which for the fractal dimension $D = 1.6$ and $N_{sys} = 1500$ results in densities of $10^4\,M_\odot\,pc^{-3}$ and $100\,M_\odot\,pc^{-3}$, respectively.

We evolve the simulations using the `kira` Hermite N-body integrator within the `Starlab` environment (Portegies Zwart et al. 1999, 2001) for 10 Myr, such that we comfortably exceed the current estimates of the age of the ONC ($1 - 4$ Myr, even taking into account potential age spreads, Jeffries et al. 2011; Reggiani et al. 2011; Bell et al. 2013; Beccari et al. 2017). We do not include stellar evolution in the simulations, nor do we include a background gas potential.

A summary of the different initial conditions is shown in Table 1. We run ten versions of each simulation, identical apart from the random number seed used to initialise the stellar masses, positions and velocities. The results presented in the subsequent figures are the average of the ten versions of each simulation.

3 RESULTS

The relatively wide planet–planet binaries, and their relatively small binding energies, make them susceptible to disruption in all of our simulated star-forming regions. Fig. 1 shows the evolution of the binary fraction of low-mass objects, which is defined as

$$f_{bin} = \frac{B}{S + B}, \tag{2}$$

where S is the number of singles, and B is the number of binary systems. The lines shown in Fig. 1 are for systems below the hydrogen-burning mass limit ($0.08\,M_\odot$), so do not include stellar-mass objects.

The solid black line shows the binary fraction in the dense star-forming regions where we draw the planet–planet properties from the JuMBO distributions (sim. A). In 1 Myr the destruction of planet–planet binaries is such that the binary fraction reduces from unity to 0.1. Even in the less dense
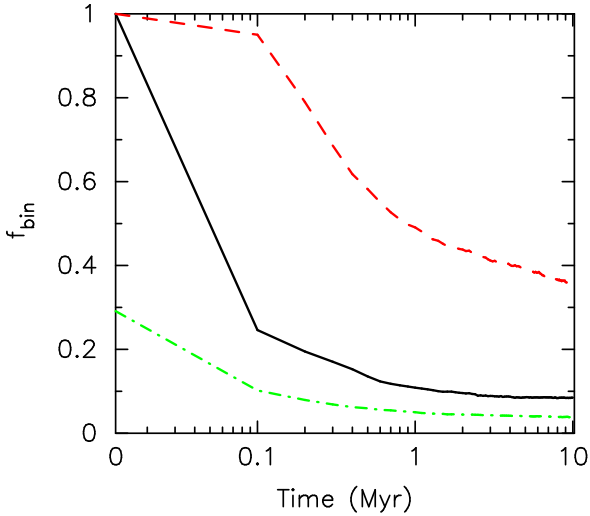
Figure 1. Evolution of the substellar-mass binary fraction (as defined in Eqn. 2) in three of our simulations. The solid black line shows the evolution of the binary fraction in our dense simulations (A). The red dashed line shows the evolution of the binary fraction in the lower-density simulations (B). The green dot-dashed line shows the evolution of the binary fraction in dense simulations that include a population of brown dwarfs drawn from the initial mass function, and so the initial binary fraction is ~ 0.3 (C). In all three of these simulations, the planet–planet separations are drawn from the JuMBO catalogue, and we have averaged together the results from ten realisations of the same initial conditions.

Figure 2. The evolution of the planet–planet binary separation distribution in N-body simulations. The open histogram shows the initial population in our N-body simulations, and the hashed histogram showns the population after 1 Myr of dynamical evolution. The solid grey histogram is the observed JuMBO distribution (Pearson & McCaughrean 2023), and the orange dot-dashed line is the fit to brown dwarf-brown dwarf binaries in the nearby Galaxy (Basri & Reiners 2006; Burgasser et al. 2007; Thies & Kroupa 2007).

star-forming regions (sim. B), the destruction of systems is significant, with the binary fraction reducing from unity to 0.5 in 1 Myr (and continuing to decrease throughout the remainder of the simulation), as shown by the red dashed line.

The green dot-dashed line shows a simulation (C) where the planet–planet binary properties are taken from the observed JuMBO distribution, but where the simulations include other substellar mass objects down to $0.01\,M_\odot$. This produces an initial binary fraction of 0.29, but the destruction of the planet–planet binaries reduces this fraction to 0.05 after 1 Myr. For clarity, we only show the simulations where the separations are drawn from the observed JuMBO distribution (A, B, C). The binary fractions in simulations where the separations are drawn from a flat distribution between 50 – 500 au (D and E) evolve in a similar manner to simulations A and B.

It is clear from these simulations that a significant proportion of the observed JuMBOs would not survive in a star-forming region with densities commensurate with the majority of nearby star-forming regions (i.e. $\geq 100\,M_\odot\,\mathrm{pc}^{-3}$). Or, to invert the statement, there must have been many more planet–planet binaries with similar properties, that have since been destroyed therough dynamical encounters, than the $\sim$40 JuMBOs presently observed in the ONC.

We now examine the effects of this dynamical destruction on the planet–planet binary separation distribution. In Fig. 2 we show histograms of the planet–planet binaries from our simulation (C) with an initial substellar binary fraction of 0.29. The open histogram is the distribution at 0 Myr, which is drawn from the observed JuMBO distribution (the solid grey histogram), but scaled upwards to reflect the many more systems we place in the simulation. The hatched histogram
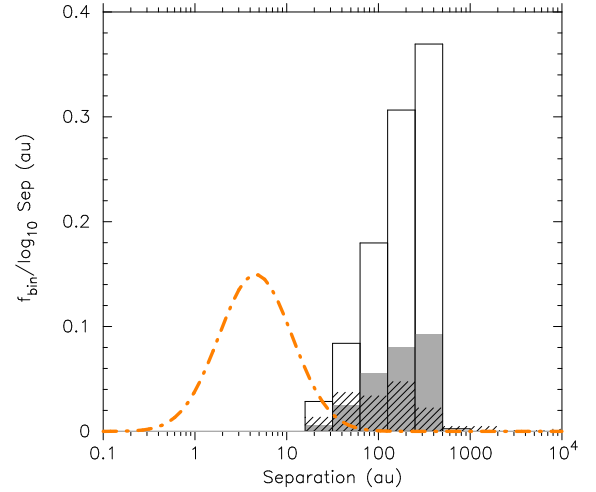
is the distribution after 1 Myr of dynamical evolution in the N-body simulation. For reference, the fit to the substellar binary distribution observed in the nearby Galaxy is shown by the orange dot-dashed line, and peaks towards much smaller separations (Basri & Reiners 2006; Burgasser et al. 2007; Thies & Kroupa 2007; Factor & Kraus 2023).

We can clearly see that the shape of the planet–planet separation distribution also changes due to dynamical interactions, with more wider systems being destroyed than the closer systems. To remove binning noise, we show the evolution of the separations as cumulative distributions in Figs. 3 and 4.

Fig. 3 shows the evolution of the separation distribution for planet–planet binaries where the initial separations are taken from the observed distribution for the JuMBOs (the solid grey line). The initial distribution in the N-body simulations is shown by the dotted black line (which is statistically identical to the observed distribution), and the distribution after 1 Myr is shown by the solid black line. For reference, the fit to the very low-mass and substellar binary separation distribution in the Galactic field is shown by the orange dot-dashed line (Basri & Reiners 2006; Burgasser et al. 2007; Thies & Kroupa 2007), which peaks at a mean separation of 4.6 au, is normalised to a binary fraction of 0.15 and is valid for systems where the primary mass is $m_P \leq 0.1\,M_\odot$ and mass ratios $q > 0.1$. In panel (a) we show the results for initially dense ($\tilde{\rho} = 10^4\,M_\odot\,\mathrm{pc}^{-3}$) star-forming regions (sim. A), and in panel (b) we show the results for lower density ($\tilde{\rho} = 10^2\,M_\odot\,\mathrm{pc}^{-3}$) star-forming regions (sim. B).

Clearly, if the stellar density during star formation in the ONC was similar to the present day (panel b), then the separation distribution does not change (but the overall fraction of planet–planet binaries will change, see the red dashed line in Fig. 1). However, if the ONC formed stars at higher densities
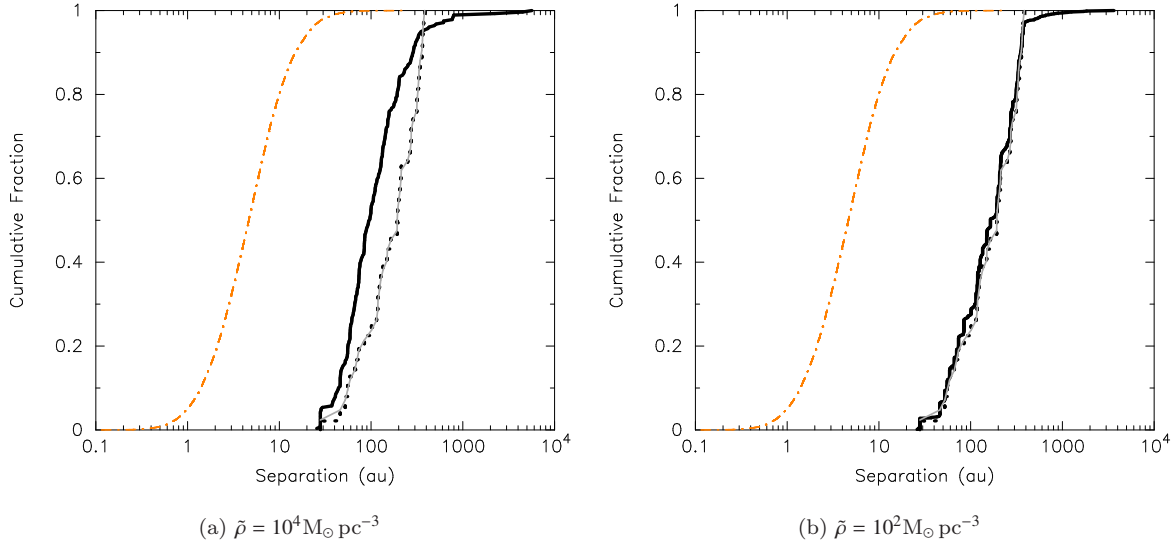
(a) $\tilde{\rho} = 10^4 \mathrm{M}_\odot \, \mathrm{pc}^{-3}$ (b) $\tilde{\rho} = 10^2 \mathrm{M}_\odot \, \mathrm{pc}^{-3}$

Figure 3. The evolution of a planet–planet binary separation distribution where the separations are drawn from the observed JuMBOs separation distribution for high (panel a) and low-density (panel b) simulations (simulations A and B, respectively). The black dotted line is the initial separation distribution, and the black solid line is the separation distribution after 1 Myr, in the *N*-body simulations. The solid grey line is the observed JuMBO distribution (Pearson & McCaughrean 2023), and the orange dot-dashed line is the fit to brown dwarf-brown dwarf binaries in the nearby Galaxy (Basri & Reiners 2006; Burgasser et al. 2007; Thies & Kroupa 2007).
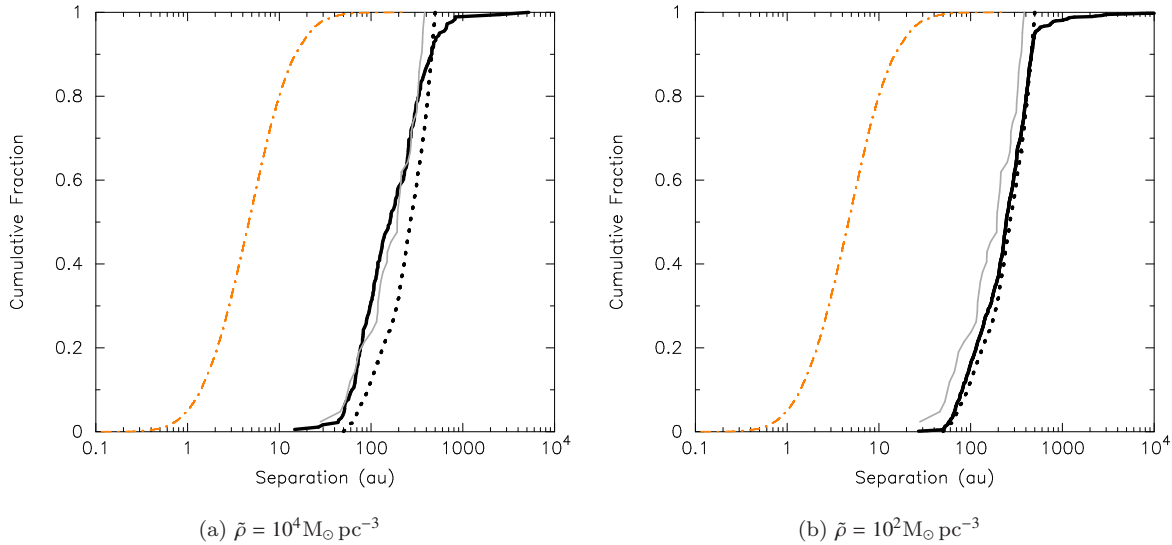

(a) $\tilde{\rho} = 10^4 \mathrm{M}_\odot \, \mathrm{pc}^{-3}$ (b) $\tilde{\rho} = 10^2 \mathrm{M}_\odot \, \mathrm{pc}^{-3}$

Figure 4. The evolution of a planet–planet binary separation distribution where the separations are drawn from a flat distribution in the range 50 – 500 au for high (panel a) and low-density (panel b) simulations (simulations D and E, respectively). The black dotted line is the initial separation distribution, and the black solid line is the separation distribution after 1 Myr, in the *N*-body simulations. The solid grey line is the observed JuMBO distribution (Pearson & McCaughrean 2023), and the orange dot-dashed line is the fit to brown dwarf-brown dwarf binaries in the nearby Galaxy (Basri & Reiners 2006; Burgasser et al. 2007; Thies & Kroupa 2007).

than observed today, then the observed JuMBO distribution today cannot be the initial distribution, as many wider systems are destroyed, moving the overall distribution to shorter separations.

If the observed JuMBOs formed with a wider range of separations (e.g. 50 – 500 au), then in a dense star-forming region the destruction of more of the wider systems processes the initial population to shorter systems (Fig. 4, where the lines are as in Fig. 3). For this initial separation distribution, dynam-

ical processing in dense regions (sim. D, Fig. 4(a)) would reproduce the observed JuMBO distribution, whereas dynamical processing in lower-density regions (sim. E, Fig. 4(b)) would leave too many wider systems.

Regardless of the initial separation distribution, it is clear that a star-forming environment with a density similar to many nearby star-forming regions ($\geq 100 \mathrm{M}_\odot \, \mathrm{pc}^{-3}$) would destroy many planet–planet binary systems with similar properties to the observed JuMBOs. This implies that even more

systems than the 42 reported in Pearson & McCaughrean (2023) would need to form, given the final binary fraction of 0.5 even in our lower-density simulations.

We also note that the observed distribution (the grey histogram in Fig. 2) shows an increasing trend to higher separations. This suggests that there may be even more wider JuMBOs that are not observed due to observational incompleteness, and these wider systems would be even more susceptible to dynamical destruction than the observed systems. If the data are incomplete, this implies that even more JuMBOs need to be produced by some formation mechanism(s) than our dynamical constraints suggest.

4 CONCLUSIONS

We present *N*-body simulations of the evolution of star-forming regions in which we place a population of planet–planet binary systems with properties similar to the JuMBOs observed in the ONC (Pearson & McCaughrean 2023) to determine how many of these systems are affected by dynamical evolution in star-forming regions. Our conclusions are as follows:

(i) The relatively wide separations (10s to 100s au), combined with their low binding energies (due to their low masses) means that many planet–planet mass binaries are destroyed in our simulations. For the present-day density of the ONC, at least half of all systems are destroyed, but for the much more likely denser initial conditions for the ONC, up to 90 per cent of these binaries are destroyed.

(ii) The implication of this high destruction rate is that to explain he observed population of 42 JuMBOs, a significantly higher number of primordial systems must have been present in the star-forming region, as many of these would be broken apart by dynamical encounters.

(iii) If the initial density of the ONC is high ($\sim 10^4\,\mathrm{M_\odot\,pc^{-3}}$), then the observed JuMBO separation distribution has been dynamically sculpted, and the initial distribution would contain significant numbers of wider systems (up to 500 au). If the inital density is lower ($\sim 100\,\mathrm{M_\odot\,pc^{-3}}$) then the observed JuMBO separation distribution is similar to the initial separation distribution.

If the observed JuMBO population are planetary mass members of the ONC (see Luhman 2024, for an alternative explanation) then the primordial JuMBO systems must have been even more numerous than they are now, suggesting they are likely to be the end-point of photoerosion of the cores of objects that would otherwise have gone on to form the more commonly occuring stellar multiple systems (Diamond & Parker 2024). Such a scenario is supported by radio observations of candidate JuMBO 24 by Rodriguez et al. (2025), who find a poper motion velocity for this system of <6 km s⁻¹, which Rodriguez et al. (2025) argue is commensurate with the velocities of stars, rather than ejected planets (Coleman 2024) (although ejected planets can have proper motion velocities much lower than this, Parker & Alves de Oliveira 2023).

DATA AVAILABILITY STATEMENT

The data used to produce the plots in this paper will be shared on reasonable request to the corresponding author.

REFERENCES

Allison R. J., Goodwin S. P., Parker R. J., Portegies Zwart S. F., de Grijs R., 2010, MNRAS, 407, 1098
André P., Di Francesco J., Ward-Thompson D., Inutsuka S.-I., Pudritz R. E., Pineda J. E., 2014, Protostars and Planets VI, pp 27–51
Basri G., Reiners A., 2006, AJ, 132, 663
Bate M. R., 2009, MNRAS, 392, 590
Beccari G., et al., 2017, A&A, 604, A22
Bell C. P. M., Naylor T., Mayne N. J., Jeffries R. D., Littlefair S. P., 2013, MNRAS, 434, 806
Burgasser A. J., Reid I. N., Siegler N., Close L., Allen P., Lowrance P., Gizis J., 2007, in Reipurth B., Jewitt D., Keil K., eds, Protostars and Planets V. pp 427–441
Cartwright A., Whitworth A. P., 2004, MNRAS, 348, 589
Coleman G. A. L., 2024, MNRAS, 530, 630
Daffern-Powell E. C., Parker R. J., 2020, MNRAS, 493, 4925
Dale J. E., Ercolano B., Bonnell I. A., 2012, MNRAS, 424, 377
Diamond J. L., Parker R. J., 2024, ApJ, 975, 204
Factor S. M., Kraus A. L., 2023, AJ, 165, 130
Foster J. B., et al., 2015, ApJ, 799, 136
Girichidis P., Federrath C., Banerjee R., Klessen R. S., 2011, MNRAS, 413, 2741
Gomez M., Hartmann L., Kenyon S. J., Hewitt R., 1993, AJ, 105, 1927
Goodwin S. P., Whitworth A. P., 2004, A&A, 413, 929
Hacar A., Tafalla M., Kauffmann J., Kovács A., 2013, A&A, 554, A55
Henshaw J. D., et al., 2016, MNRAS, 457, 2675
Jeffries R. D., Littlefair S. P., Naylor T., Mayne N. J., 2011, MNRAS, 418, 1948
King R. R., Parker R. J., Patience J., Goodwin S. P., 2012, MNRAS, 421, 2025
Kroupa P., Petr M. G., McCaughrean M. J., 1999, New Astronomy, 4, 495
Kuznetsova A., Hartmann L., Ballesteros-Paredes J., 2015, ApJ, 815, 27
Langeveld A. B., et al., 2024, AJ, 168, 179
Larson R. B., 1981, MNRAS, 194, 809
Lazzoni C., Rice K., Zurlo A., Hinkley S., Desidera S., 2024, MNRAS, 527, 3837
Li G., Adams F. C., 2015, MNRAS, 448, 344
Li D., Mustill A. J., Davies M. B., 2020, MNRAS, 499, 1212
Luhman K. L., 2024, AJ, 168, 230
Luhman K. L., et al., 2024a, AJ, 167, 5
Luhman K. L., Alves de Oliveira C., Baraffe I., Chabrier G., Geballe T. R., Parker R. J., Pendleton Y. J., Tremblin P., 2024b, AJ, 167, 19
Marks M., Kroupa P., 2012, A&A, 543, A8
Maschberger T., 2013, MNRAS, 429, 1725
McCaughrean M. J., Pearson S. G., 2023, arXiv e-prints, p. arXiv:2310.03552
Myers P. C., 2011, ApJ, 735, 82
Parker R. J., 2014, MNRAS, 445, 4037

Parker R. J., 2023, MNRAS, 525, 2907

Parker R. J., Alves de Oliveira C., 2023, MNRAS, 525, 1677

Parker R. J., Goodwin S. P., 2011, MNRAS, 411, 891

Parker R. J., Goodwin S. P., Allison R. J., 2011, MNRAS, 418, 2565

Parker R. J., Wright N. J., Goodwin S. P., Meyer M. R., 2014, MNRAS, 438, 620

Pearson S. G., McCaughrean M. J., 2023, arXiv e-prints, p. arXiv:2310.01231

Portegies Zwart S., Hochart E., 2024, SciPost Astronomy, 3, 001

Portegies Zwart S. F., Makino J., McMillan S. L. W., Hut P., 1999, A&A, 348, 117

Portegies Zwart S. F., McMillan S. L. W., Hut P., Makino J., 2001, MNRAS, 321, 199

Reggiani M., Robberto M., Da Rio N., Meyer M. R., Soderblom D. R., Ricci L., 2011, A&A, 534, A83

Rodriguez L. F., Loinard L., Zapata L., Ortiz-Leon G. N., 2025, arXiv e-prints, p. arXiv:2504.15519

Salpeter E. E., 1955, ApJ, 121, 161

Sánchez N., Alfaro E. J., 2009, ApJ, 696, 2086

Schmeja S., Klessen R. S., 2006, A&A, 449, 151

Schoettler C., de Bruijne J., Vaher E., Parker R. J., 2020, MNRAS, 495, 3104

Thies I., Kroupa P., 2007, ApJ, 671, 767

Vázquez-Semadeni E., Palau A., Ballesteros-Paredes J., Gómez G. C., Zamora-Avilés M., 2019, MNRAS, 490, 3061

Wang Y., Perna R., Zhu Z., 2024, Nature Astronomy, 8, 756

Whitworth A. P., Zinnecker H., 2004, A&A, 427, 299